Supporting Information

Ni-doping induced phase transition and electron evolution in cobalt hexacyanoferrate as a stable cathode for sodium ion batteries

Junjie Quan[a], Enze Xu[a], Hanwen Zhu[a], Yajing Chang[b], Yi Zhu[a], Pengcheng Li[a], Zhenjie Sun[a], Dabin Yu[b], Yang Jiang[a,*].

[a]School of Materials Science and Engineering and, Hefei University of Technology, 230009, Hefei, People's Republic of China

[b]State Key Laboratory of Pulsed Power Laser Technology, National University of Defense Technology, 230037, Hefei, People's Republic of China

Corresponding authors' E-mail: apjiang@hfut.edu.cn; (Y. Jiang).

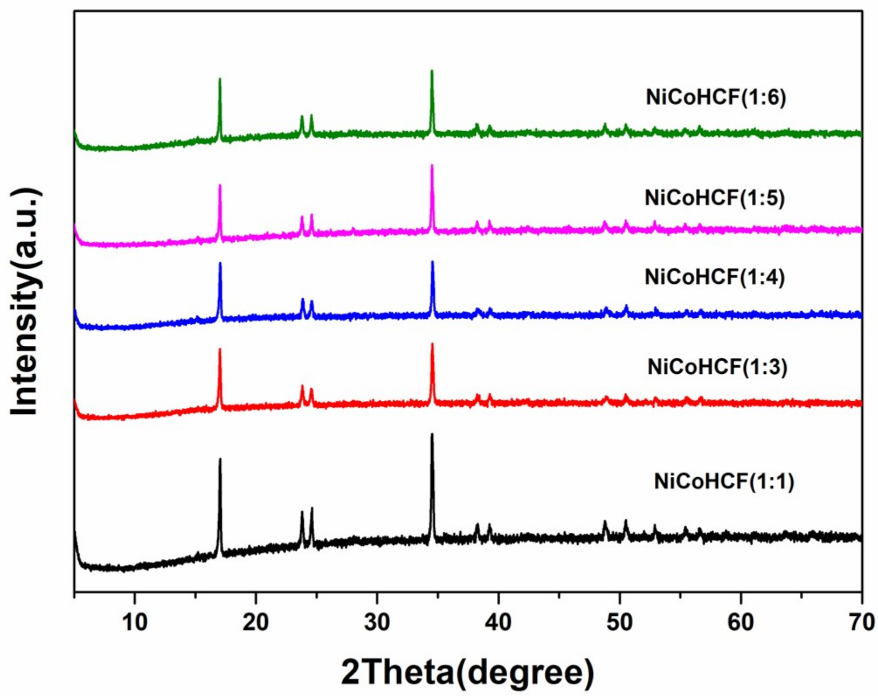

Fig. S1 XRD of NiCoHCF with different ratios of Nickel and Cobalt.

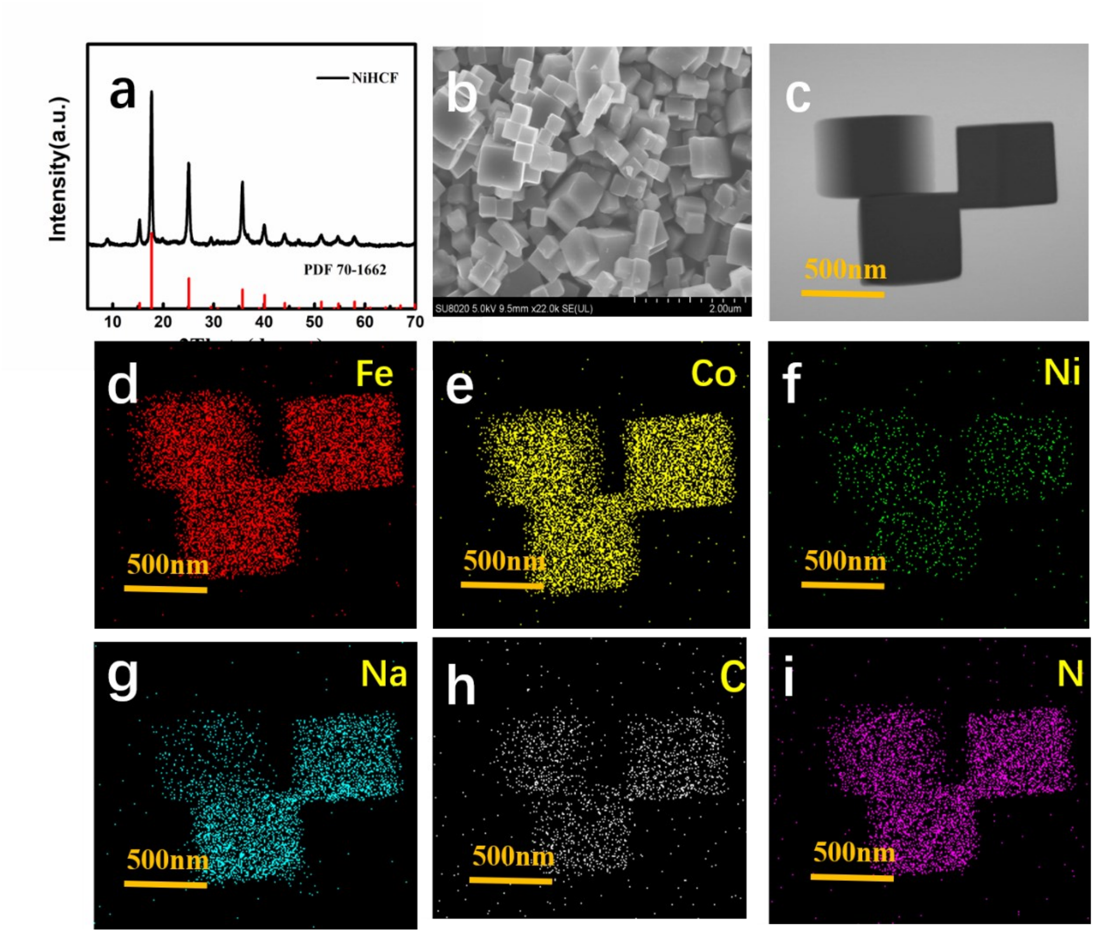

Fig. S2 (a) xrd pattern of NiHCF. (b) SEM image of CoHCF. (c-i) TEM image and corresponding Elemental mapping images of NCHCF.

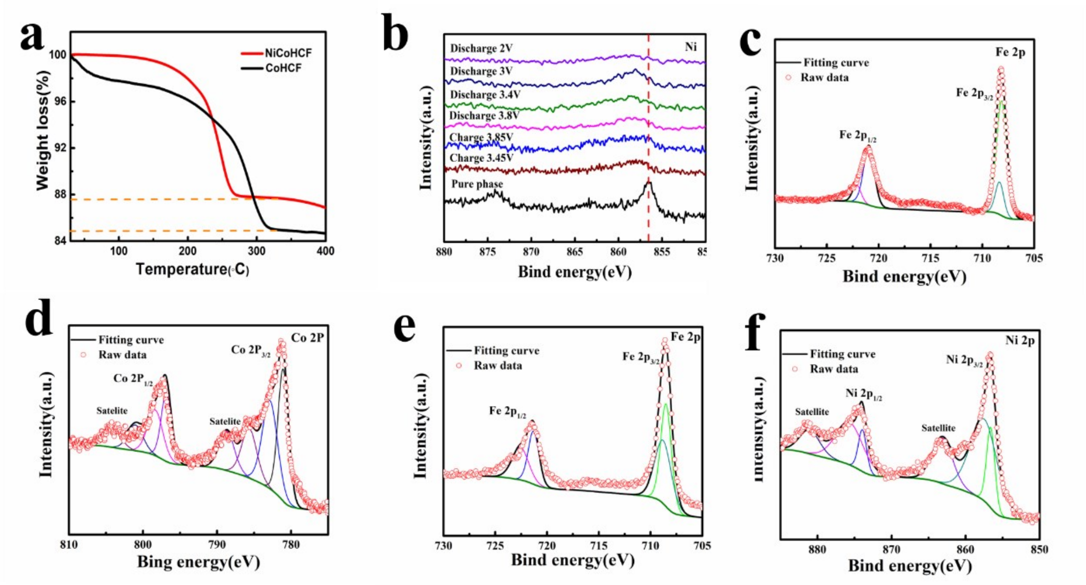

Fig. S3 (a) TGA curves of CoHCF and NCHCF. (b) XPS spectra of Ni in NCHCF. (c, d) Fe 2p, Co 2p XPS spectrum of CoHCF. (e, f) Fe 2p, Ni 2p XPS spectrum of CoHCF.

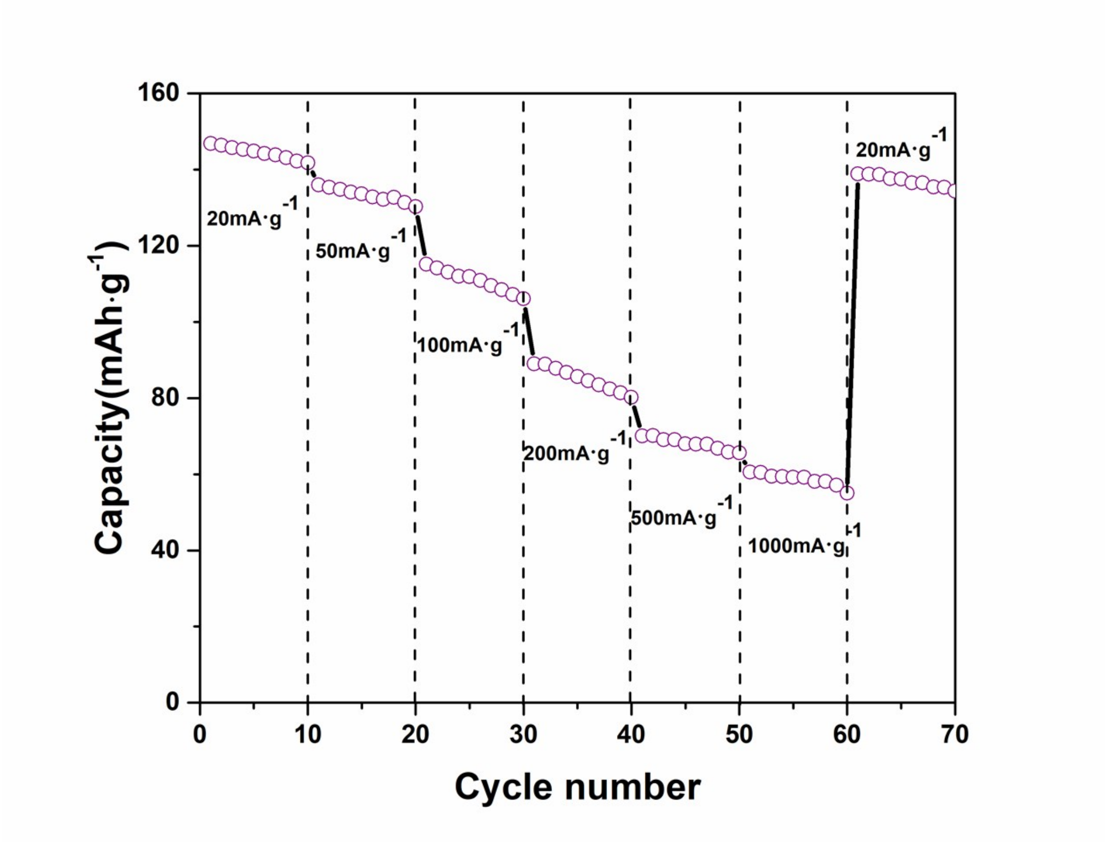

Fig. S4 Rate performance of CoHCF.

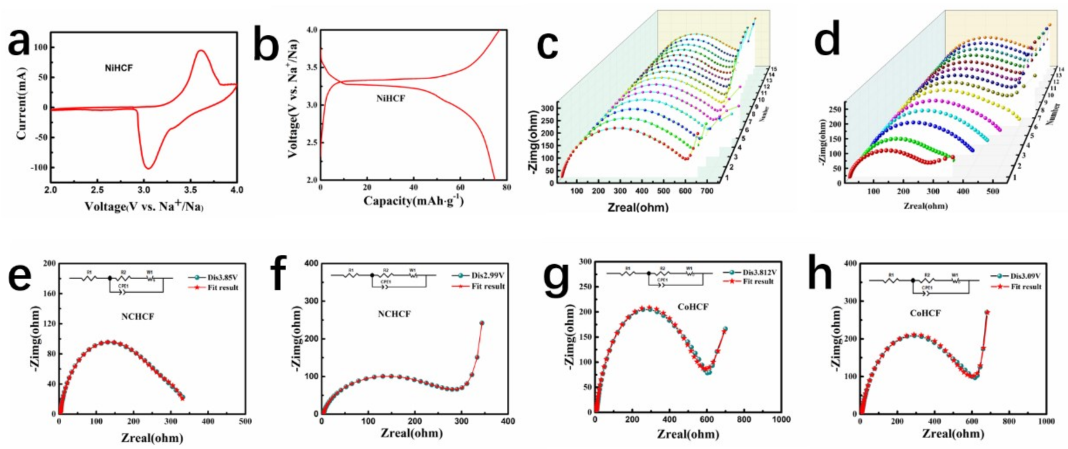

Fig. S5 CV curve (a) and charge-discharge profile (b) of NiHCF. In-situ EIS of CoHCF(c) and NCHCF(d) during the first discharging process. (e-h) Nyquist profile and fitting curve of CoHCF and NCHCF.

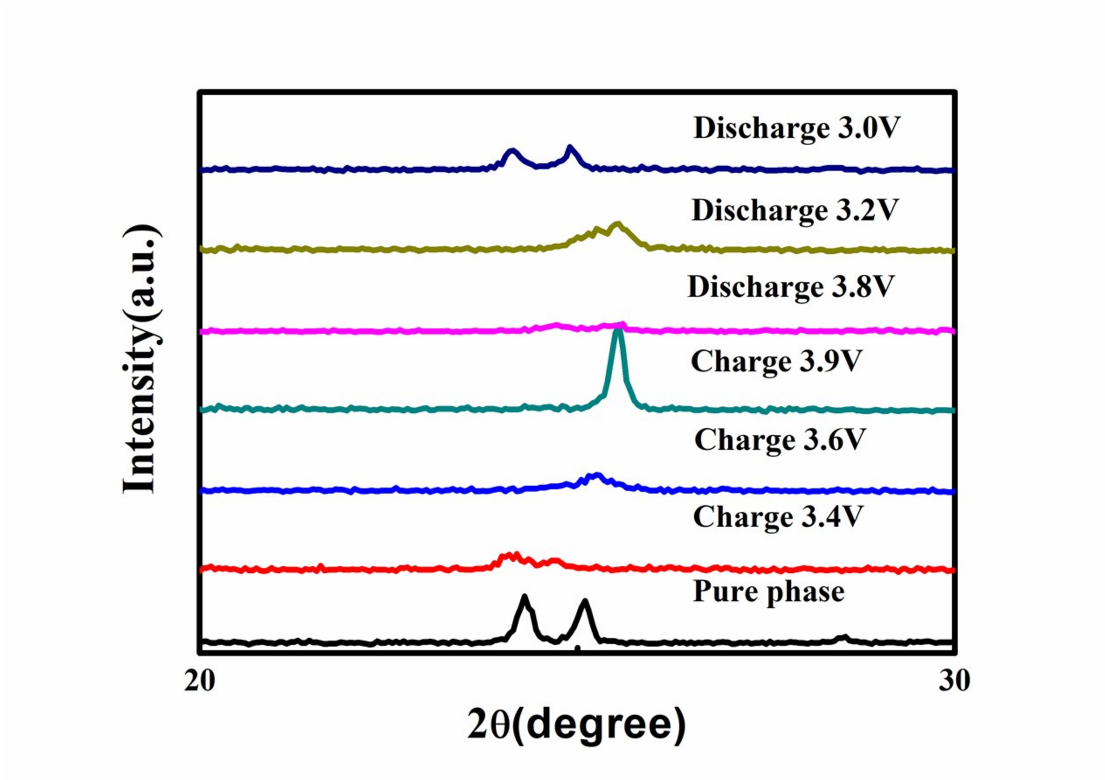

Fig. S6 XRD of NiCoHCF with different ratios of Nickel and Cobalt.

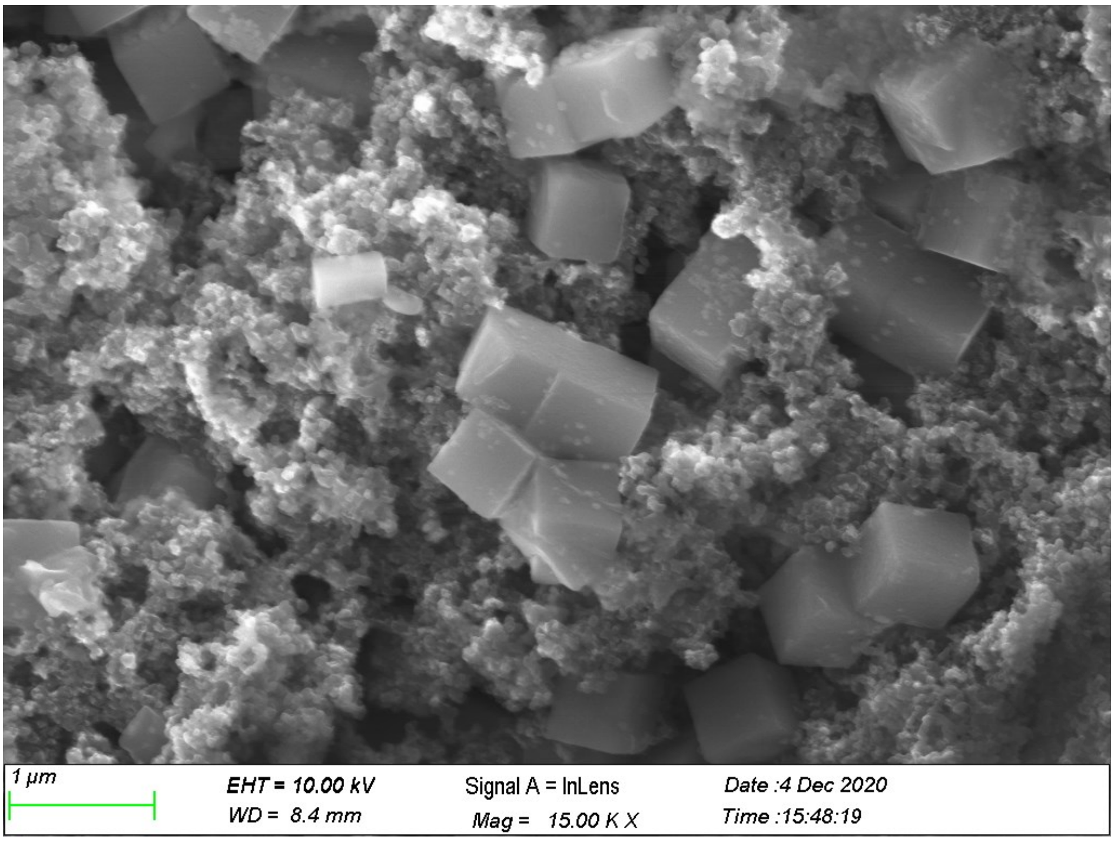

Fig. S7 The SEM image of NiCoHCF electrode after 10 cycles at100mA·g^{-1}

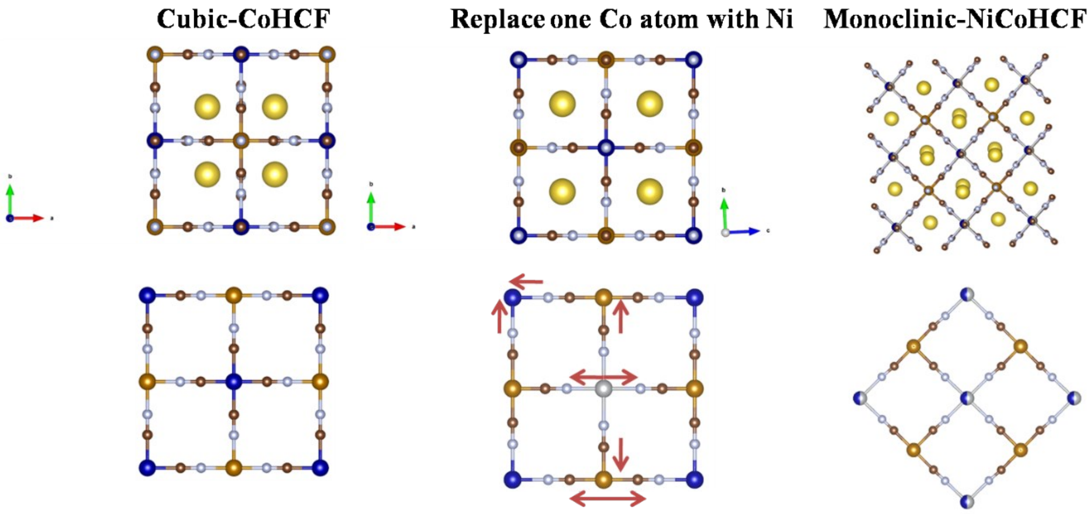

Fig. S8 bond length change during nickel substitution

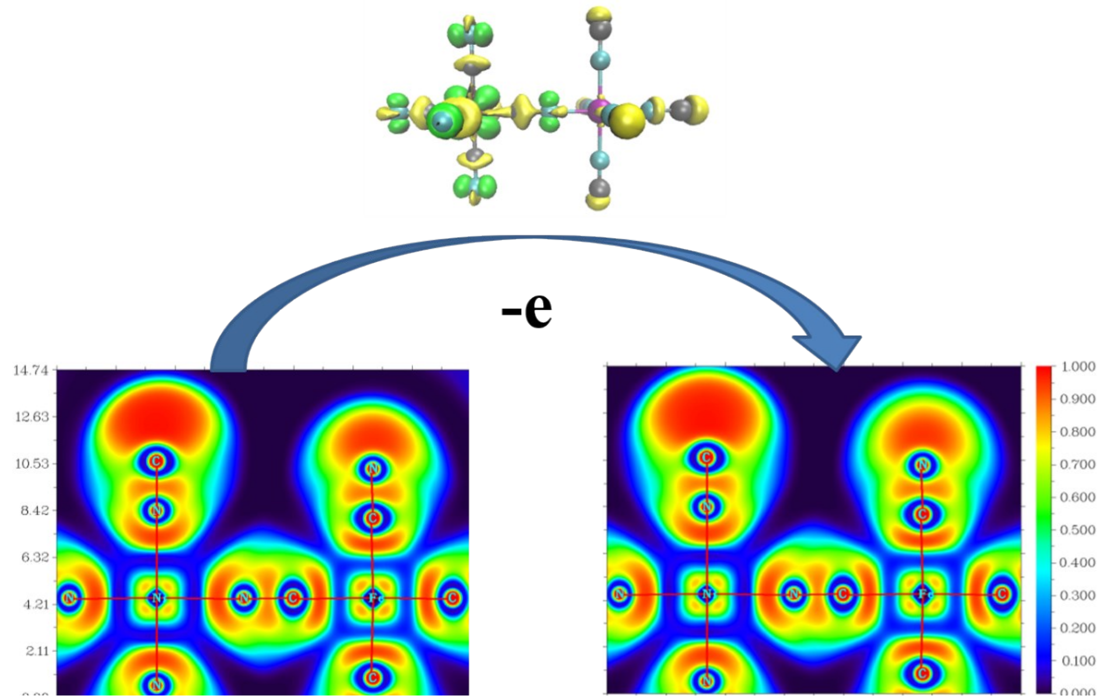

Fig. S9 Charge density difference and corresponding electron density projection drawing of NiHCF.

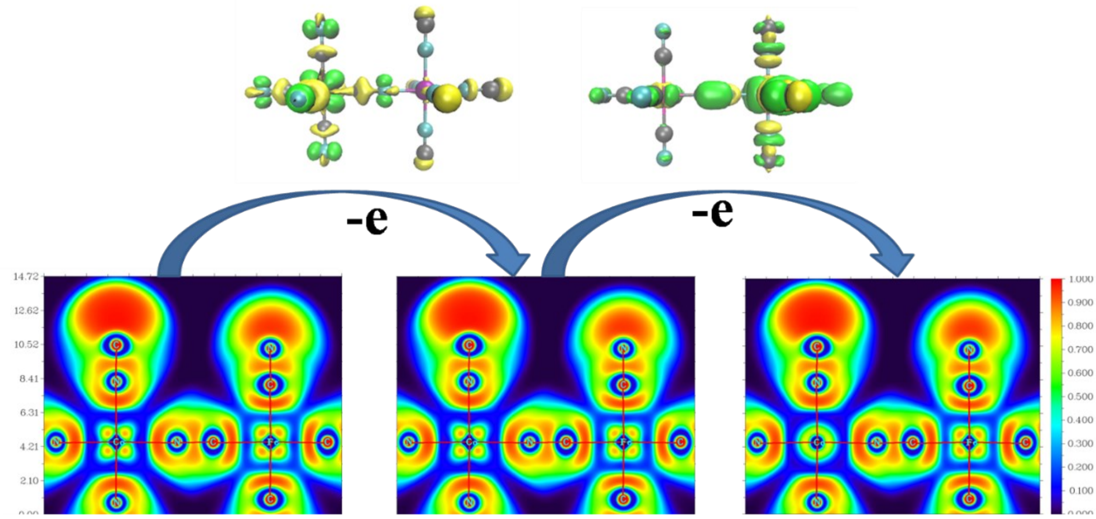

Fig. S10 Charge density difference and corresponding electron density projection drawing of CoHCF

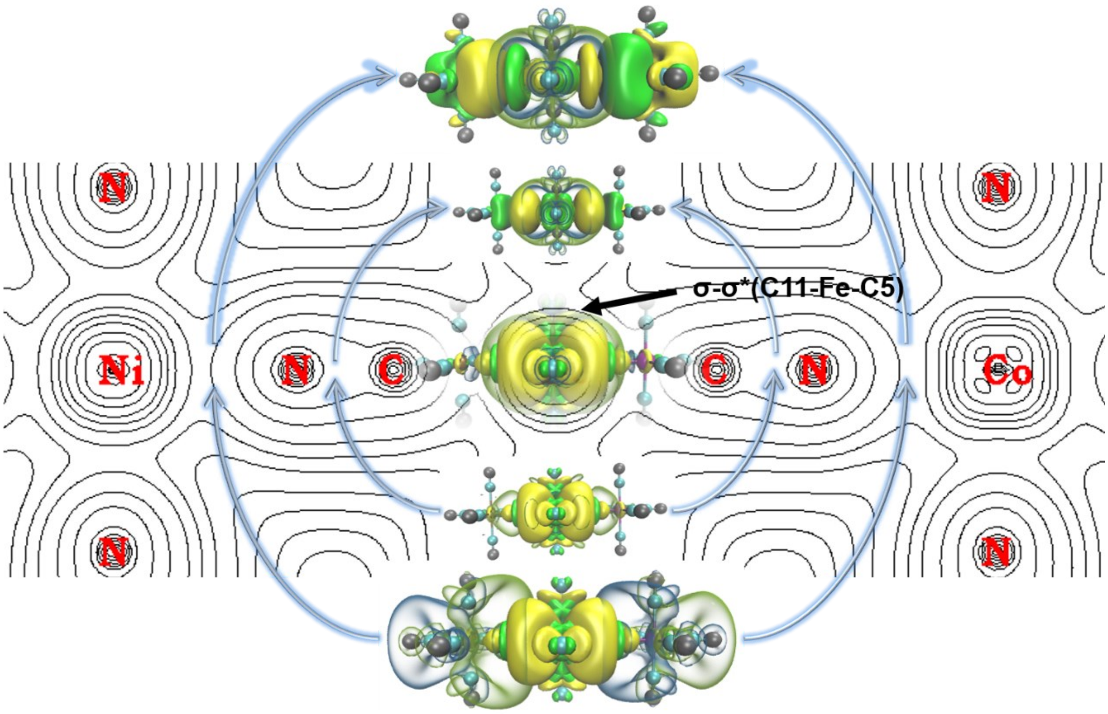

Yellow solid isosurface——Positive wave function of bonding orbital
Green solid isosurface——Negative wave function of bonding orbital
Yellow transparent isosurface——Positive wave function of Anti-bonding orbital
Blue transparent isosurface——Negative wave function of Anti-bonding orbital

Fig. S11 Wavefunction interaction between electron donor and acceptor related to Fe-C molecular orbital.

Table. S1 Element contents of CoHCF and NCHCF

sample	ICP % wt.				Elemental analysis % wt.			TG % wt.
	Na	Ni	Co	Fe	C	N	H	H2O
CoHCF	10.71		17.83	15.04	20.53	23.67	1.304	15.4
NCHCF	11.87	1.23	16.54	15.78	21.03	24.03	1.161	12.1

Table S2 Structural parameters of CoHCF, NiCoHCF from Rietveld analysis

Sample-CoHCF

Lattice parameter: a=b=c=10.24432 Å, and α=β=γ=90°

Rwp=9.2%, Rp=8.4%, χ^2=10.91

Atom	**x**	**y**	**z**	**Occupancy**	**Uiso(Å^2)**
Fe1	**0.5**	**0.5**	**0.5**	**1**	**0.0634**
Co1	**0.5**	**1**	**0.5**	**1**	**0.0712**
Na1	**0.75**	**0.75**	**0.75**	**1**	**0.0343**
O1	**0.5**	**1**	**0.725**	**0.17**	**0.0655**
N1	**0.5**	**0.7967**	**0.5**	**0.83**	**0.0872**
C1	**0.5**	**0.6848**	**0.5**	**1**	**0.0521**

Sample NCHCF

Lattice parameter: a=10.44307 Å, b=7.43999 Å, c=7.21542 Å, α=β=γ=90° and γ=91.95639°

Rwp=5.3%, Rp=4.6%, χ^2=5.64

Atom	**x**	**y**	**z**	**Occupancy**	**Uiso(Å^2)**
Fe1	**0.5**	**0**	**1**	**1**	**0.0085**
Ni1	**0.5**	**0.5**	**0.5**	**0.3**	**0.0079**

Co1	**0.5**	**0.5**	**0.5**	**0.7**	**0.0199**
Na1	**0.2658**	**0.4554**	**-0.0022**	**1**	**0.045**
O1	**0.239**	**0.2252**	**0.2636**	**1**	**0.0442**
N1	**0.5098**	**0.2969**	**0.7062**	**1**	**0.0104**
N2	**0.296**	**0.5068**	**0.5077**	**1**	**0.0101**
N3	**0.5031**	**0.2944**	**0.2972**	**1**	**0.0119**
C1	**0.5126**	**0.181**	**0.8085**	**1**	**0.0141**
C2	**0.1869**	**0.5115**	**0.5101**	**1**	**0.0118**
C3	**0.504**	**0.1848**	**0.1895**	**1**	**0.0167**

Table. S3 Value of bond length

	Ni-N(Å)	Co-N(Å)	(Fe-C)≡N-Ni(Å)	(Fe-C)≡NCo(Å)
NCHCF	2.04774	1.95481	1.80671	1.89028
CoHCF		1.9742		1.86835

Table. S4 Sodium ion insertion voltage of CoHCF and NCHCF

Voltage / Sample	Na0→Na1	Na1→Na2	Na2→Na3
CoHCF	3.81	2.84	
NCHCF	3.85	2.97	2.42

Table S5 Interaction energy between donor orbital and acceptor orbital

Donor orbital	Acceptor orbital	E(2)/kcal·mol^{-1}	E(j)-E(i)/a.u.	F(I,j)/a.u.
σ(Fe1-C5)	**σ* (Fe1-C5)**	**10.19**	**1.28**	**0.146**
	σ* (Co2-N4)	**6.93**	**0.78**	**0.094**
	π*(N4-C5)	**2.94**	**1.65**	**0.091**
σ(Fe1-C11)	**σ* (Fe1-C11)**	**13.30**	**1.25**	**0.165**
	σ* (Ni3-N10)	**6.47**	**0.86**	**0.097**
	π* (N10-C11)	**3.02**	**1.66**	**0.092**
σ(Co2-N4)	**σ* (Fe1-C5)**	**2.11**	**1.34**	**0.068**
	σ* (Co2-N4)	**4.21**	**0.84**	**0.075**
	π*(N4-C5)	**0.81**	**1.71**	**0.048**
σ(Ni3-N10)	**σ* (Fe1-C11)**	**2.53**	**1.31**	**0.074**
	σ* (Ni3-N10)	**1.45**	**0.92**	**0.046**
	π* (N10-C11)	**1.45**	**1.72**	**0.063**
π(N4-C5)	**σ* (Fe1-C5)**	**3.10**	**1.88**	**0.098**
	σ* (Co2-N4)	**3.48**	**1.37**	**0.088**
π(N10-C11)	**σ* (Fe1-C11)**	**3.72**	**1.85**	**0.107**
	σ* (Ni3-N10)	**2.63**	**1.45**	**0.078**

Table. S6 The reported PBA materials in the literature

Sample	Charge/discharge plateaus	Reversible capacity	Rate capability	Refs.
NaNiCoFe(CN)6	3.92/3.71V,3.62/3.18V,3.45/2.98V	146mAh·g^{-1} at 20mA·g^{-1}	105mAh·g^{-1} at 1A·g^{-1}	This work
$Na_{1.95}Fe[Fe(CN)_6]_{0.93}$	3.76/3.53V, 3.02/2.87V	160 mAh·g^{-1} at 50mA·g^{-1}	60 mAh·g^{-1} at 1.6A·g^{-1}	1
$Na_{0.22}Ni[Fe(CN)_6]_{0.76}$	3.315/3.314V	78 mAh·g^{-1} at 17 mA·g^{-1}	57.5 mAh·g^{1} at 4250 mA·g^{-1}	2
$NaCoFe(CN)_6$	3.89/3.73V,3.42/3.12V	148 mAh·g^{-1} at 20 mA·g^{-1}	60 mAh·g^{-1} at 500 mA·g^{-1}	3

$NaMnFe(CN)_6$	3.85/3.57V,3.52/3.27V	134 mAh·g^{-1} at 6 mA·g^{-1}	45 mAh·g^{-1} at 4800 mA·g^{-1}	4
$NaNiMnFe(CN)_6$	3.83/3.49V,3.58/3.07V	120 mAh·g^{-1} at 50 mA·g^{-1}	78 mAh·g^{-1} at 1600 mA·g^{-1}	5
$NaNiCoFe(CN)_6$	3.9/3.73V,3.4/3.04V	92 mAh·g^{-1} at 50 mA·g^{-1}	69 mAh·g^{-1} at 800 mA·g^{-1}	6

Reference:

(1) Y. You, X. Wu, Y. Yin, Y. Guo, High-quality Prussian blue crystals as superior cathode materials for room-temperature sodium-ion batteries, Energy Environ. Sci. 7 (2014) 1643-1647.

(2) Y. You, X. Yu, Y. Yin, K. Nam, Y. Guo, Sodium iron hexacyanoferrate with high Na content as a Na-rich cathode material for Na-ion batteries, Nano Res. 8 (2015) 117-128.

(3) L. Wang, J. Song, R. Qiao, L. A. Wray, M. A. Hossain, Y. Chuang, W. Yang, et. al., Rhombohedral Prussian White as Cathode for Rechargeable Sodium Ion Batteries, J. Am. Chem. Soc. 137 (2015) 2548−2554.

(4) Y. Huang, M. Xie, J. Zhang, Z. Wang, Y. Jiang, G. Xiao, et. al., A novel border-rich Prussian blue synthetized by inhibitor control as cathode for sodium ion batteries, Nano Energy 39 (2017) 273–283.

(5) X. Tang, H. Liu, D. Su, P. H. L. Notten, G. Wang, Hierarchical sodium-rich Prussian blue hollow nanospheres as high-performance cathode for sodium-ion batteries, Nano Research 11 (2018) 3979–3990.

(6) H. Hu, W. Liu, M. Zhu, Y. Lin, Y. Liu, J. Zhang, et. al., Yolk-shell Prussian blue nanoparticles with fast ion diffusion for sodium-ion battery, Materials Letters 249 (2019) 206–209.